



# Aptian–Albian shale oil unconventional system as registration of Cretaceous oceanic anoxic sub-events in the southern Tethys (Bir M'Cherga basin, Tunisia)

Rachida Talbi<sup>1</sup> · Rached Lakhdar<sup>2</sup> · Amor Smati<sup>1</sup> · Reginal Spiller<sup>3</sup> · Raymond Levey<sup>4</sup>

Received: 5 April 2018 / Accepted: 2 November 2018 / Published online: 16 November 2018  
© The Author(s) 2018, corrected publication 2019

## Abstract

The Bir M'Cherga basin (North-east Tunisia), with about 600 km<sup>2</sup> area, had recorded four Middle Cretaceous source rocks well stratigraphically correlated with the four known oceanic anoxic sub-events: OAE1a, OAE1b, OAE1c, and OAE1d. Variety of lithology, thickness and organic richness had characterized these source rocks. The sedimentary tectonic analysis, the petrology and geochemistry study established the petroleum system of these source rocks. Basin formation began early in the Barremian–Aptian interval by synsedimentary tectonics reactivating old basement faults. During the Aptian–Albian, the formed basin had a depocenter that recorded thicker black shales while its NW and SE edges remained raised under the Triassic halokinetic activities. The evolution of the sedimentary filling during this period generated two sedimentary cycles corresponding to two filling second-order fining and thickening upwards sequences. The black shales that constitute these source rocks are formed between subtidal and external platform environment and are interbedded with juxtaposed high organic rich layers and poor ones. The rich organic facies consists of dark shale that constitutes the source rock. The poor organic beds formed by light grey and nodular limestones constitute an intra host reservoir. Thereby, petroleum system consists in an “unconventional oil shale hybrid systems with a combination of juxtaposed organic-rich and organic-lean intervals associated to open fractures”. The kerogen is essentially amorphous, with marine planktonic origin and low ligneous organic matter contribution. This organic material of dark facies had been well preserved in an anoxic environment with little or no energy. Light grey limestones were of oxic-to-sub-oxic environment. The stage of the thermal evolution for these source rocks provided by  $IH/T_{max}$  diagram is of the “oil window”. The average transformation ratio (TR) is estimated as 45% suggesting thus black shales are oil shale resources which still close about untransformed 55% of its hydrocarbon generating potential. The expulsion and release of oil into these source rocks are proven by the observation of hydrocarbons filling micro-cracks and by the variable values of the oil saturation index OSI ranging from 0 to 138%. The latter exceeds 100% near the paleo-high reliefs indicating two “oil crossover” areas attributed to the high degree of oil source rock saturation and accumulation of hydrocarbons considered ideal for hydraulic fracturing. This oil crossover is a consequence of secondary migration into black shale source rock, achieved by various faults created during the distensive phase that were reactivated again several times.

**Keyword** Biozone · Anoxic sub-event · Geodynamic · Black shales · Hydrocarbon · Petroleum system

## Introduction

Black shales are the consequence of oceanic anoxic events that had marked the geological history in the global ocean since the early Cretaceous and record the phases of

proliferation and diversification of marine biomass in sediments; which led to the genesis of good source rocks of oil and gas (Schlanger and Jenkyns 1976; Arthur et al. 1985). Most black shales were deposited during the Oceanic Anoxic Event OAE1 of the Middle Cretaceous and coincide with the unfolding of global phenomena related to the main phases of mid-ocean volcanism, generalizing transgressions and increasing CO<sub>2</sub> levels in the atmosphere (Schlanger and Jenkyns 1976; Arthur et al. 1985).

✉ Rachida Talbi  
rachorg235@gmail.com

Extended author information available on the last page of the article

This Oceanic Anoxic Event occurred over a long period (113–109 Ma) with short-term paroxysms ( $\leq 1$  Ma) that coincided with the accumulation and fossilization of significant amounts of organic matter in four black shale units during the four oceanic anoxic sub-events: OAE1a, OAE1b, OAE1c and OAE1d (Jenkyns et al. 1990; Bralower et al. 1994; Jarvis et al. 2002; Leckie et al. 2002; Soua 2016). The first marker (OAE1a) is of the Barremian–Aptian boundary identified by *Schackoina cabri* and *Globigerinelloides blowi* biozone (Weissert et al. 1998; Sliter 1989; Bralower et al. 1994) particularly in the south of France: the “Goguel level” formation of Br  h  ret (1994) and in Italy: the “Selli level” formation of Coccioni and Galeotti (1994). The second sub-event (OAE1b) is of the Lower Albian with *Ticinella bejaouaensis* and *Hedbergella planispira* biozone, characterizes the western Tethyan (Br  h  ret 1994; Bralower et al. 1994). This interval is marked by a glaciation phase of the latest Aptian followed by an eustatic rise phase during the Lower Albian (Weissert et al. 1998). The third sub-event (OAE1c) of basal Upper Albian is indicated by *Biticinella breggiensis* biozone, and has been identified in central Italy, in inner western USA and in Australia (Bralower et al. 1994; Coccioni and Galeotti 1993; Haig and Lynch 1993; Erbacher et al. 1996). Finally, the sub-event OAE1d is of latest Upper Albian with *Rotalipora appenninica* biozone and is widely represented across the Tethys Ocean but sporadically represented in the southern part of the Atlantic and Indian Ocean and the eastern part of the Pacific ocean (Br  h  ret 1994; Erbacher et al. 1996; Wilson and Norris 2001; Bornemann et al. 2017).

We emphasize that those four oceanic anoxic sub-events of the Middle Cretaceous have never been encountered together in the same basin. The Bir M’Cherga basin in the north-east of Tunisia is an exception and offers a unique opportunity to analyze and correlate them. Elsewhere, in the rest of the “Tunisian furrow” bordering the southern Tethyan domain, the main three sub-events (OAE1a, b, and d) had been identified and correlated with their counterparts of the global ocean (Soua 2016) while oceanic anoxic sub-event OAE1c, had never been reported in this area.

This study aims to highlight the coexistence of the four sub-events OAE1a, OAE1b, OAE1c, and OAE1d and to correlate them with the anoxic sub-events of the global ocean. The tectono-sedimentary analysis would make it possible to understand the role played by local factors in the creation of anoxic conditions and to define the type of petroleum system that can be attributed to those source rocks. On another side, success in the exploration and exploitation of shale gas and oil resources is attracting increasing interest in oil production from organic-rich mudstones or black shales. The economic value of petroleum liquids is becoming greater than that of natural gas (Jarvie 2012). Thus, black shales with high residual petroleum potential can be revised as shale oil

and gas resource systems to extract hydrocarbons stored in the source rock.

To achieve this objective, it becomes necessary to identify the dominant organic, petrologic and geodynamic criteria to characterize the oil system of the source rocks that were deposited during these four oceanic anoxic sub-events.

## Geologic and stratigraphic settings

### Geodynamic setting of the Bir M’Cherga basin

The Aptian–Albian interval corresponds, in northern Tunisia and particularly in Bir M’Cherga basin (Fig. 1a–c), to the deposit of sedimentary marlstone, limestone and grey-black laminated limestone with a maximum thickness of around 1000 m: “Fahd  ne formation” (Burolet 1956; Jauzein 1957: unpublished work). This sequence was deposited in an open and relatively deep subsiding paleogeographical domain in northern Tunisia: the “Tunisian Furrow” or “Atlas basin” (Bolze et al. 1952).

Several authors suggest the existence of a close link between tectonics and paleogeography in Tunisia (Boltenhagen 1981; Chikhaoui and Turki 1995). In particular, they note from the Lower to Middle Cretaceous that syn-sedimentary tectonics fragmented the sedimentary floor of the basin (Boltenhagen 1981; Chihi 1995) into a series of tilted blocks that emerged at the beginning of the Aptian interval (Fig. 2a). An extensive tectonic regime that occurred in northern Tunisia during this period was oriented NE–SW nearby E–W faults including those bordering the southern part of the Atlas basin. This controlled the gradual collapse of the “Tunisian Furrow” by the subsidence and tilting blocks in an E–W orientation (Figs. 1c, 2b). A half-graben structure generated sedimentary micro-basins, created at subsiding blocks, characterized by thick sedimentary prisms on the collapsed side of normal faults. Reduced ones were built on their resistant side. The raised edges of these micro-basins show mismatches and breaches of dismantling (Martinez et al. 1991; Ellouz 1984; Chikhaoui and Turki 1995). During this time volcanic events also accompanied sedimentation, particularly in the platform–basin transition area where NW–SE rifting (crustal thinning) was located at Enfidaville, the Sahel and the Pelagian Sea (Fig. 2a) (Raaf and Althuis 1952; Laaridi-Ouazaa 1994). The studied area corresponds to a NW boundary basin under a Cretaceous distensive regime preferentially during the change of the sequences (Boltenhagen 1981; Laridhi-Ouazaa 1994; Illies 1981). The Bir M’Cherga basin (Figs. 1c, 2b) falls within this scope and was located at the East-northeastern end of this Tunisian furrow during the Barremian–Albian interval.

This basin was an intracratonic feature that corresponded to a regional extension graben (Figs. 1c, 2b), delimited by

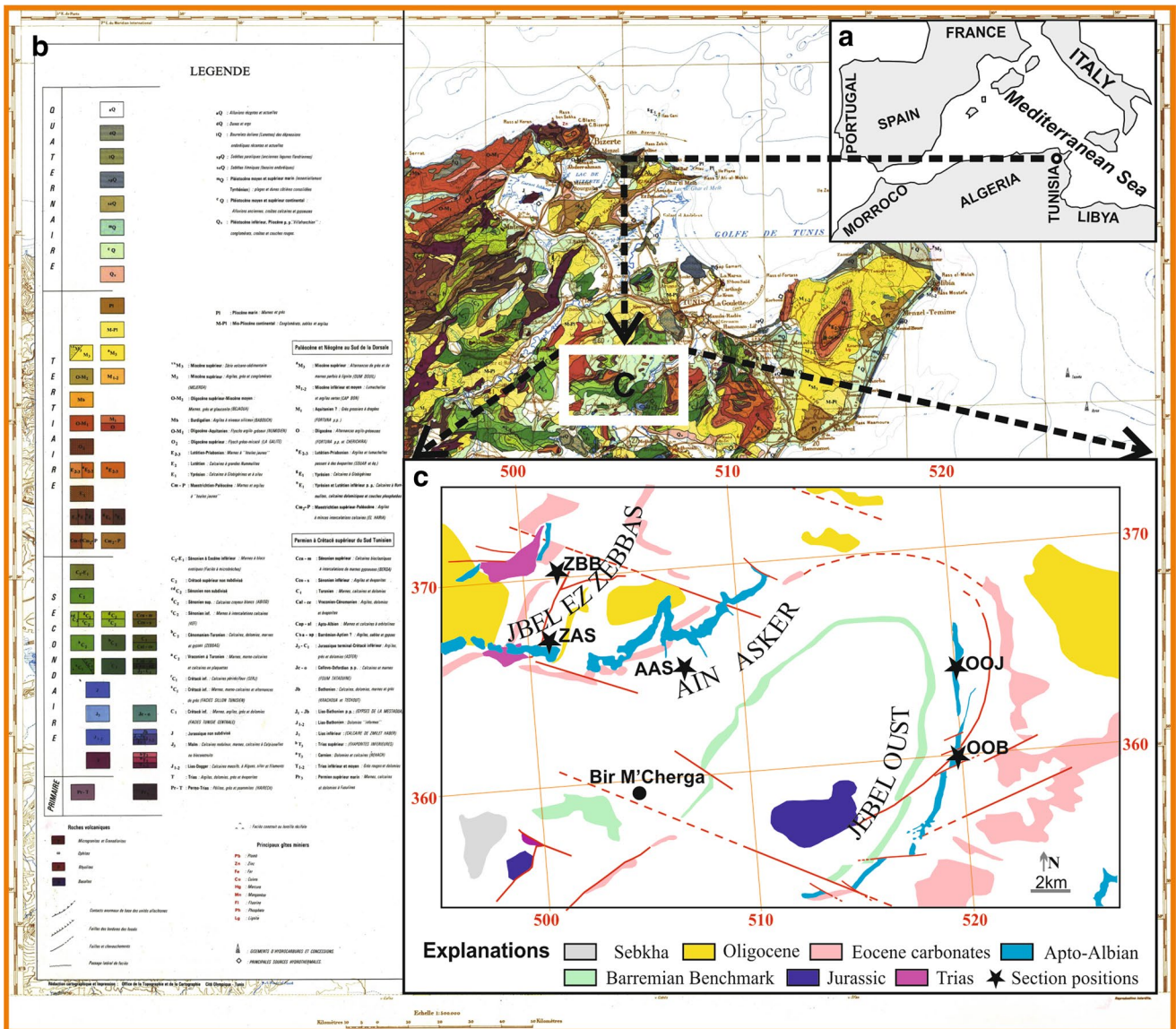


**Fig. 1** a Geographic regional situation; b north-east Tunisian geologic map and c simplified geologic map of study area (Bir M'Chergua) showing section locations (Corel Draw figure exported into jpeg format)

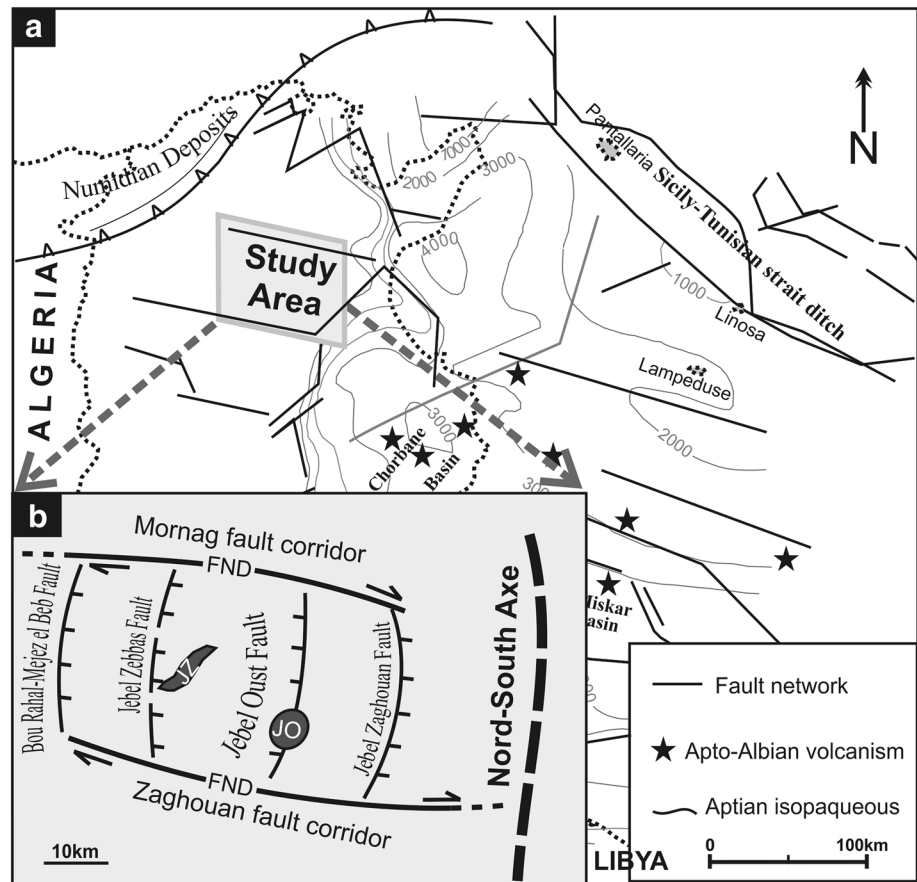
NNE-SSW and NW-SE normal faults that extended into the basement. Starting in the Upper Jurassic, the graben collapsed and was filled with a thick sedimentary sandstone and pelitic sequence during the Neocomian–Barremian interval (Burollet 1956; Jauzein 1957). The top Barremian–Aptian period marks an extensive tectonic phase which reactivates the movements of the basement into horsts, grabens and tilted blocks. The Triassic dome pierces the overlying sedimentary cover intersecting sub-meridian faults with NW-SE oriented ones. The NW-SE extension faults are regional and define the northern and southern boundary of the Bir M'Cherga graben (Figs. 1c, 2b).

These faults expose prominent resistant blocks such as those of Jebel Zebbas and Djebel Oust (Figs. 1c, 2b). Thus, a

condensed area within the sedimentary section can be characterized during the Bedoulian-Gargasian interval (Memmi 1989) and precede the first filling phase of the basin during the Aptian–Albian interval. The NW-SE extensional tectonic activity also involves the deposition of a marly limestone that covers the latest Lower Albian and that is characterized throughout the entire basin by little variations in thickness and lithology (Talbi 1991) (Fig. 8). During the transition from the Lower Albian to the Upper Albian, halokinetic movements associated with the Triassic section were favored by the reactivation of paleo-basement faults (Smati 1986). This increases the paleo-relief maintaining the basin's old architecture inherited from the Jurassic phase. During the latest Upper Albian, those paleo-highs become gradually



**Fig. 2** **a** Aptian main structural elements of Tunisian showing study area (Boltenhagen 1981; redrawn); **b** schematic structural map of study area (Corel Draw figure exported into jpeg format)



invaded by sedimentation associated with extensional tectonic faults. Significant thickness variations characterized the marlstone of the lower Upper Albian (Fig. 8). However, the latest Upper Albian shows minimal variations of thickness (Burolet 1956; Jauzein 1957).

## Lithostratigraphic units

The filling Bir M'Cherga graben consisted in a thick sandstone and pelite sedimentation of the Neocomian–Barremian interval underlying the Aptian–Albian marly sequence containing black shales. Sedimentation began with a series of marls which contained two banks of laminated limestone dated back to the Barremian–Aptian by *schackoina cabri* biozone (Memmi 1989, 2014).

The base of the Aptian is represented by olive-green ammonite-rich silty clays marked locally by glauconite with frequent yellow siliciclastic thin beds. At this time, the structural architecture of the basin was marked by tilted blocks on the normal E-W faults side. A thick sedimentary sequence with pelagic fauna filled the collapsed areas, whereas the condensed series of reduced thickness are typical of outer-shelf and peritidal setting on resistant blocks.

Barremian–Aptian black shales are settled beside the top of resistant block in Oued Bou Hejba (OOB section) near Jebel Oust. The deposition of these black shales announces the beginning of the anoxic Aptian–Albian crisis.

The depositional hiatus marking the Aptian–Albian unconformity is probably induced by the tectonic phase that occurred at the end of the Aptian in relation to halokinetic movements characterizing the region (Memmi 1989). Here, we find a missing deposition located on the top of the paleo-highs built upon Triassic domes. The deeper Albian facies is everywhere represented by the same lithological sequence consisting on grey-black marls with frequent black shales horizons. The early Lower Albian is represented by grey marlstone becoming laminated towards the top. The latest Lower Albian corresponds to a dominant carbonate deposit enriched at the base by laminated limestones, in the middle by marlstones and at the top by bioturbated nodular thickening limestones. A rich microfauna containing *Ticinella primula* biozone characterizes this sub-unit. The lower Upper Albian is represented by a marlstone showing few layers of laminated limestones with a rich ammonites and belemnites fauna. This sub-unit is characterized by *Biticinella breggiensis*. The terminal Upper Albian is dated by *Planomalina buxtorfi* biozone. It is characterized

by laminated limestones at resistant paleo-high areas and interbedded laminated limestones with marls at relatively deep ones (Jauzein 1957; Talbi 1991).

Significant variations in thickness characterize especially the marl series of the basal Albian and those of the basal Upper Albian (Fig. 6). This can be attributed to extensive tectonic phases reactivating paleo-faults starting at Barremian–Aptian passage and at the latest Lower Albian. This sedimentary rupture is marked by the appearance of spherical gypsum nodules and secondary sulfates, characterizing the passage Lower Albian–Upper Albian. Those are becoming more common in the direction of resistant wrinkles (Fig. 6) (Talbi 1991).

During the latest Upper Albian, the paleo-reliefs created at the latest Lower Albian will gradually be invaded by sedimentation in an extensional tectonic setting. Black shales are settled on the paleo-reliefs of Jebel Zebbas (ZAS) and Djebel Oust (OOJ) whereas interbedded marlstones and limestones, with thin black shale levels, are formed at Ain Asker (AAS) and Oued Bou Hejba (OOB), in the deeper areas of the basin (Talbi 1991).

At the Cenomanian–Upper Albian limit, halokinetic pulsations are reactivated again. The transgressive Cenomanian marlstones are generally discordant on the Upper Albian sediments (Figs. 6, 7). Then spherical gypsum nodules and secondary sulfates have scored this discordance near the paleo-reliefs. Indeed, the top of the Upper Albian black shales is showing an erosive surface in AAS and OOB sections; whereas in ZAS and OOJ sections they are partially truncated by faults. While in ZBB section, these black shales had removed completely (Jauzein 1957; Talbi 1991).

### Filling sequence and associated black shales

In the Bir M'Cherga basin, the Aptian–Albian sediments are organized in two filling second order fining and thickening upwards sequences with organic-rich marlstones and limestones that form black shales. A mineral paragenesis of these facies is represented by about 50–70% of calcite, 20–40% of silica, 0–9% of feldspars and 6–12% of clays. According to Dunham (1962) classification, calcareous sediments are of packstone-to-wackstone microfacies (Talbi 1991).

The first sequence corresponds to the Aptian–Lower Albian interval and consists of two sedimentary members. The first member begins by two black shales indicating Barremian–Aptian transition which are related to OAE1a and are overlain by Upper Aptian olive-green clays and basal Lower Albian grey marlstones. The latter are enriched with pelagic fauna containing, especially pyritic ammonites. The second member is represented by thick black shales corresponding to OAE1b interbedded with nodular limestone becoming thicker and bioturbated at the top (Fig. 6).

The second sequence is Upper Albian age. Its lower boundary is marked by spherical gypsum nodules and barytine. This sequence consists also two members. Its basal one is represented by grey marlstones containing rich ammonites and belemnites fossils. Those marlstones are interbedded with thin black shales assigned to OAE1c in the basin center (AAS) and in its SE side (OOB and OOJ). The second member of this sequence is represented by black shales interbedded with thin nodular limestones corresponding to OAE1d upon paleo-highs. Those black shales are interbedded with relatively thick marlstones and limestones in the deeper basin area (Fig. 6).

Tectonosedimentary analysis shows that each sequence is delimited by two major distensive tectonic phases controlled by halokinetic activity (Perthuisot et al. 1988). Each phase destabilizes the sedimentary floor and creates inequalities of the relief. A pelagic subtidal sedimentation occurs in collapsed areas and an external platform deposits characterize high areas. Black shales accumulated during the four oceanic anoxic sub-events characterize an intermediate environment between subtidal and external platform since they are located between pelagic faunal marls and bioturbated nodular limestones (Fig. 7).

The correlation of these sedimentary sequences with the documented regional eustatic cycles (Marie et al. 1982; Memmi 1989) show that each sequence coincides with the beginning of a regional eustatic cycle whose paroxysm corresponds to the black shale deposits (Fig. 6). Each eustatic cycle, as a result of an extensional tectonic phase, starts by the marlstone deposits before the installation of the anoxic phase that allows black shales deposits. Then, the sequence ends by oxic-to-sub-oxic sediments. The regional eustatic cycle coincides perfectly with the global chart of Vail et al. (1977) as shown by the Fig. 6.

### Materials and methods

Five geological sections have been excavated in the Bir M'Cherga basin (Fig. 2). The samples collected were first dated using planktonic microfauna.

Total rock geochemistry analysis was conducted on 317 rock samples using a Carmograph 8 WOSTHOFF and a Rock-Eval II. The total organic carbon (TOC) is carried out by burning the sample at 1100 °C under an oxidizing atmosphere after carbonates destruction. This technical method (Espitalié et al. 1977) measures the compounds released by organic matter pyrolysis of 100 mg of sediment under an inert atmosphere (Helium) and by programming the heating temperature from 180 to 600 °C at a rate of 25 °C/mn. A pyrogram showing three peaks related to three organic compounds is provided: the S1 and S2 peaks correspond, respectively, to the free hydrocarbon quantities released

at 180 °C and to the potential hydrocarbons obtained by thermal cracking of the insoluble organic matter (kerogen) at a temperature ranging between 180 and 600 °C. The S3 peak represents the organic oxygen compounds. Finally, the maximum temperature ( $T_{max}$ ) measured at the top of the S2 corresponds to the kerogen thermal maturity degree. Several parameters are calculated from S1, S2, and S3 such as the hydrogen index ( $HI = (S2 \times 100)/TOC$  in mg HC/g TOC), the oxygen index ( $O = (S2 \times 100)/TOC$  in mg  $CO_2/g$  TOC), the hydrocarbon generation potential ( $HGP = S1 + S2$ ) and the oil saturation index ( $OSI = (100 \times S1)/TOC$ ).

Liquid chromatography was performed on bitumen extracted from 32 rock samples using an organic solvent (Dichloromethane:  $CH_2Cl_2$ ). The extract fractionation is carried out according to the separation protocol SARA. First, it is passed through a column containing an amalgam of copper and zinc to separate the asphalenes from the maltenes. The latter are divided into three compounds, namely saturated hydrocarbons which are eluted with heptane, aromatics with a 2/1 mixture volume of *n*-heptane and toluene and finally the resins with a 1/1/1 mixture volume of dichloromethane, toluene and methanol. The saturated fraction obtained was subsequently analyzed by gas chromatography on a Carlo-Erba apparatus “5880 series gas chromatograph”, equipped with a capillary column SP 2100 of 30 m × 0.25 mm, by programming temperature from 80 to 300 °C at a rate of 5°C/mn.

Optical study was realized by scanning electron microscopy then by microscopic reflection, transparency and fluorescence with an Ortholux microscope and a Cerchar photometer. This was conducted on 25 samples of polished rocks and organic matter concentrates. The preparation technique for the concentrate organic matter was performed according to the method described by Bertrand and Pradier (1993). About 200 g of crushed rock is centrifuged in a dense solution ( $d = 1.7$ ) and the supernatant is recovered on a sieve. The organic particles of the concentrate are subsequently fixed on a suitable resin and then subjected to polishing.

## Results

### Petrographical and geochemical characterization of the organic matter

#### Organic matter constituents

Petrographic organic microfacies analysis interests two types of facies: organic-rich laminated limestones (dark shales) and poor organic nodular limestones (light grey facies). Those two types of facies are interbedded in black shales. The dark shales are organic-rich thin micro-beds (Fig. 3a) showing sometimes well-preserved fish scales (Fig. 3b)

and microfauna filled with bitumens (Fig. 3c). Abundant nanoplanktonic fauna, especially coccoliths are shown by SEM in the clear thin micro-beds constituting the dark facies (Fig. 3d). However, light grey facies do not show laminated structures but hydrocarbons filling micro-fractures (Figs. 3f, 4e). Dark facies are rich autogenic fromboidal pyrite crystals (Fig. 3g) characterizing most of source rocks kerogens (Tissot and Welte 1984).

Organic matter extracted from dark black shales show essentially amorphous type (Fig. 3h). But those from light grey facies are constituted by rarefied oxidized ligneous fragments: fusinites (Fig. 3i, j).

All these microfacies show an intragranular initial porosity formed by the cavities or lodges of the microfauna and the nannofauna (Fig. 3c, d) associated with an intergranular porosity similar to that developed between the fromboidal pyrite crystals (Fig. 3g). To this primary porosity is added another secondary represented by microfracture (Fig. 3e, f).

### Geochemical results

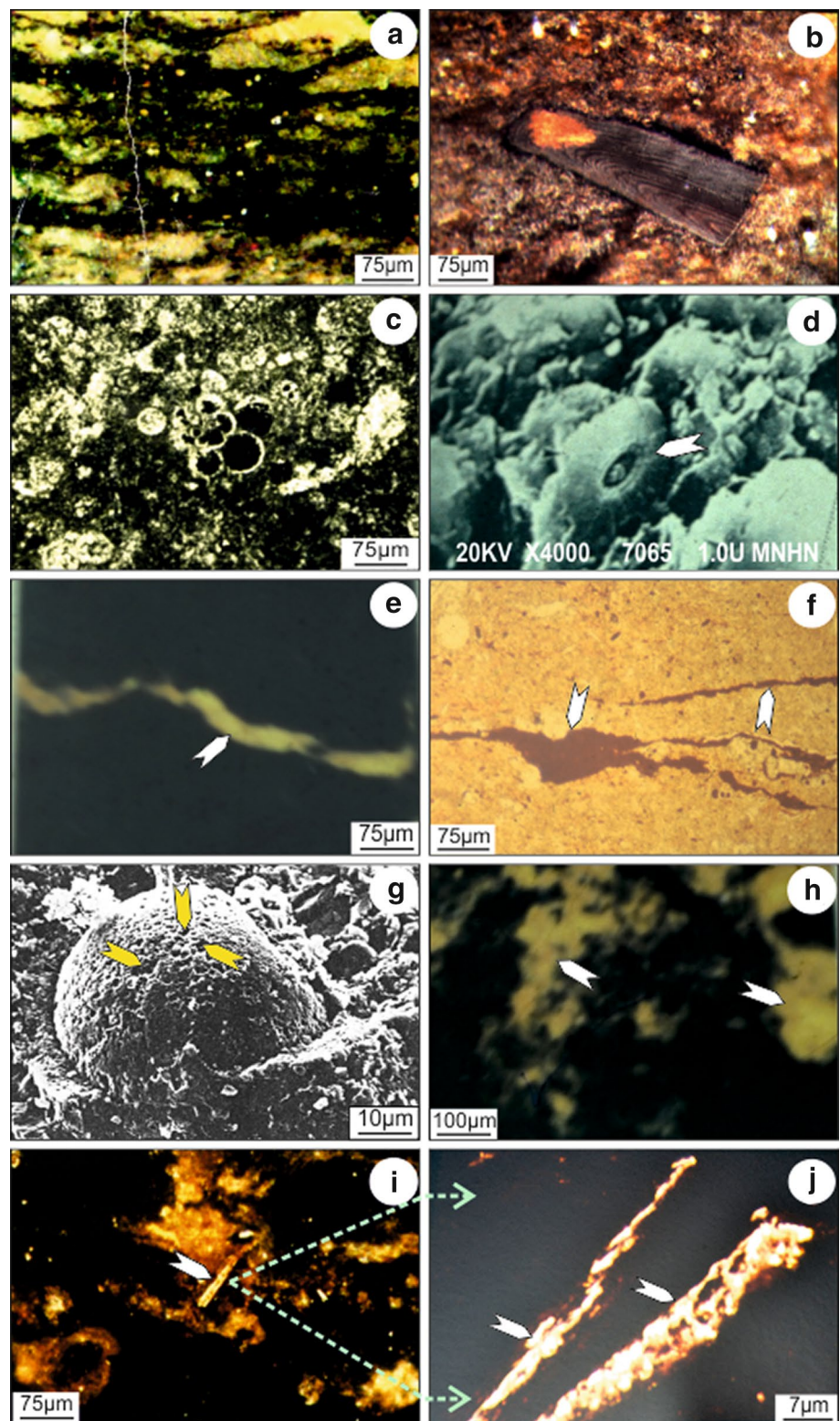
Organic matter analysis results range from 0.1 to 13.91 wt% TOC (Table 1). Dark shales recorded more than 1 wt% TOC and light grey limestones recorded less than 0.5 wt% TOC. Marls are generally with intermediate contents. Average TOC contents/section range between 0.55 and 2.19 wt%. The average values of hydrocarbons generative potential HGP ( $S1 + S2$ ), hydrogen index HI and oxygen index OI, range, respectively, from 1.41 to 25.49 kg HC/t rock for HGP, 178 to 347 mg HC/g TOC for HI and 25 to 194 for OI (Table 1). These large dispersion values may be related to the filling environment that oscillated between oxic, sub-oxic, and euxinic conditions. Dark shales are the euxinic filling environment. But light grey limestone and marlstone are sub-oxic-to-oxic deposits.

The kerogen origin is determined by the HI/OI diagram (Fig. 4) (Espitalié et al. 1977) showing that most of the representative sample points (about 70%) occur along lines I and II corresponding, respectively, to sapropelic and marine planktonic organic matter. Ligneous organic particles do not exceed 5% estimated referring to the petrographical analysis and about 30% of type IV ( $OI \geq 100$ ) that can be related to thermal and weathering alteration of type I and II initials organic deposits (Fig. 4). Note that most type I origin samples are from ZAS section which records the highest TOC contents (13,91wt%) and the highest HI/OI ratio (= 14) (Table 1).

The analysis of the composition of the dichloromethane extract kerogen shows the percentages of saturated and aromatic hydrocarbons ranging, respectively, from 9 to 37% and from 4 to 10%. Heavy compounds range from 56 to 73% for resins and 0 to 13% for asphaltens (Table 2).



**Fig. 3** Organic-rich and organic-lean microfacies and their micro-constituents of Bir M’Cherga Aptian–Albian source rocks (Corel Draw figure exported into jpeg format). **a** Laminated organic matter with about 14 wt% TOC (thin rock section—transmitted light), **b** preserved fish scale (thin rock section—Reflected light), **c** microfacies with planktonic fauna showing intragranular microporosity filled by hydrocarbons (thin rock section—transmitted light), **d** Coccolithes-rich nanofacies showing intragranular fossil porosity (SEM photo), **e** Hydrocarbons filling microfractures with 0.75 wt% TOC (thin rock section—fluorescent light), **f** hydrocarbons filling microfracture (thin rock section—transmitted light), **g** framboidal pyrite showing intragranular nanoporosity between crystals (rock section—SEM photo), **h** amorphous organic matter (extracted organic matter—fluorescent light), **i** fusinite fragment (extracted organic matter—reflected light) and **j** detail of **i**



The low asphaltene and the high resin fractions of dichloromethane extract denote the good oil quality. In fact, the resinous compounds can be transformed entirely into hydrocarbons, while asphaltene release only a tiny

fraction by thermal cracking. Such result attests, usually on a low maturity degree since the source rock starts generating heavy bitumen in the early stage of organic matter cracking.

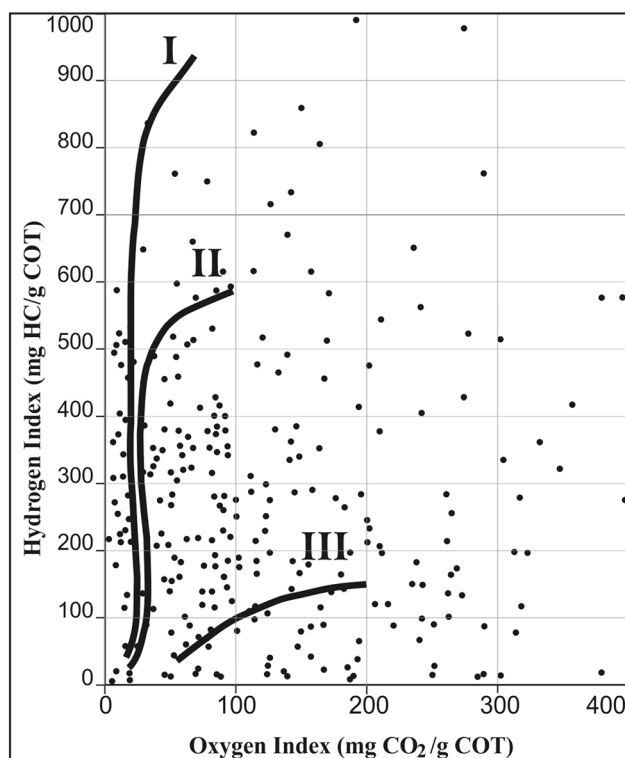


**Fig. 4** HI/OI diagram showing the representative points of samples from Bir M'Cherga Aptian–Albian source rocks (Corel Draw figure exported into jpeg format)

The mode of the *n*-alkane distribution of saturated hydrocarbons being around  $C_{17}$ – $C_{18}$  and located between  $C_{14}$  and  $C_{20}$  (Table 2) and the disappearance of the *n*-alkanes with a length hydrocarbon molecules in the  $C_{25}$ – $C_{35}$  range is attributed to a biomass originated from marine planktonic organic matter (Durand 1993). The absence of an impurity of the *n*-alkanes (Fig. 5) is attributed to mature sediment. But developed hump in some chromatograms under  $C_{25}$ – $C_{35}$  (Fig. 5b) can be related to a strong biodegradation which characterizes the extracted samples from the top of the sequence (Fig. 6). In fact the hump is related to naphthenic hydrocarbons which derived from bacteria activity at sediment–water interfaces (Durand 1993) and may characterize oxic-to-sub-oxic sediment deposits.

#### Organic-rich and organic-poor facies environment deposit

Petrographic and geochemical study carried out on selected samples shows that the two juxtaposed microfacies into black shale constitute interbedded source rocks and reservoirs. Laminated dark shale records the highest organic content with amorphous marine compound constituting the source rock kerogen. By thermal cracking, the kerogen

releases hydrocarbons which fill the inter- and intra-source rock pores. Hydrocarbons migrate through microfractures and impregnate the underlying and the overlying light grey beds constituting reservoirs. Poor asphaltenes and rich resin hydrocarbons may result from a first generation of oil and reflect a low degree of maturity corresponding at least to the beginning of “the oil window”.

Moreover, well-conserved organic materials indicate low energy and anoxic conditions with a reduced euxinic environment (Goy 1979). The high degree of preservation is related to the high organic matter accumulation in the dark facies and indicates the high degree of euxinic conditions by early-formed framboidal pyrite under water–sediment interface (Schieber and Gordon 2001). On the other hand, light grey facies characterize sub-anoxic-to-oxic environment, where at the top of the sequence they become bioturbated and indicate the end of the anoxic cycle.

#### Anoxic sub-events and associated source rocks

The sedimentological and geochemical spatiotemporal analysis of organic matter richness of the Bir M'Cherga Aptian–Albian series led to distinguish three important organic-rich black shale levels that constitute good source rocks. These latter correspond to the three sub-events OAE1a, OAE1b, and OAE1d (Fig. 6). A fourth and less expressed one may be related to OAE1c.

The first anoxic sub-event appears at the Barremian–Aptian limit and is referred to the *schackoina cabria* biozone. It is represented by two black shale levels that are approximately 7 m thick near Jebel Oust area (OOB) and contain an average organic material contents: 0.80 wt% for TOC, 222 mgHC/g for HI, and 3.13 kg HC/t for GHP with maximum values, respectively, of 2.95, 728, and 3.13 (Table 1; Fig. 6). This sub-event identified in Tunisia for the first time by Talbi (1991) was manifested in the Center, the North and the North-East of Tunisia and covering a vast paleogeographic domain. OAE1a event is characterized by a diachronic and a clear variation of TOC richness and thickness confirmed by Soua (2016). This oceanic anoxic sub-event is well documented and identified for the first time in the Italian Apennines as “Livello Selli” OAE1a (Coccioni and Galeotti 1994).

The second oceanic anoxic sub-event (OAE1b) is of Lower Albian age dated by *Ticinella primula* biozone. It consists of black shale levels from 75 to 210 m thick with homogeneous organic material contents. The average geochemical data values are 0.70 wt% for TOC, 294 for HI, and 2.35 kg HC/t for GHP. Their maximum contents are, respectively, 2.97, 845 and 3.07 recorded at ZBB section (Table 1; Fig. 6). This OAE1b sub-event was documented in France Voconcian basin (Bréhéret 1994) and all the

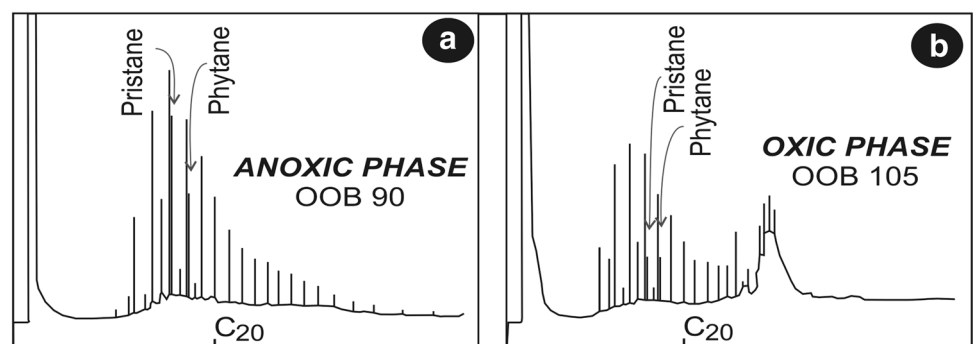


**Table 1** Average organic geochemical data recorded from TOC analysis and Rock–eval pyrolysis of Bir M’Cherga Aptian–Albian source rocks

Section	OAE	Samp. num. / thickness	Average TOC min–max	Average HGP min–max	Average HI min–max	Average OI min–max	HI/OI
ZAS	OAE1d	17/12 m	5.13 0.46–13.91	25.49 0.01–74.18	347 39–508	25 5–82	14
	OAE1c	14/15 m	0.64 0.12–1.97	1.67 0.03–7.37	178 8–608	98 17–164	1.8
	OAE1b	55/86 m	0.81 0.10–2.95	3.13 0.06–15.63	222 60–728	72 8–366	3
ZBB	OAE1b	29/210 m	0.80 0.16–2.97	3.07 0.30–8.11	425 60–847	131 26–383	3
AAS	OAE1d	14/50 m	0.96 0.34–1.53	2.70 0.27–7.92	214 36–584	154 19–257	1.4
	OAE1c	11/72 m	0.53 0.09–1.04	1.70 0.02–3.21	231 6–990	179 81–282	1.3
	OAE1b	21/130 m	0.84 0.04–1.80	2.23 0.10–6.30	275 20–626	151 3–396	1.8
OOB	OAE1d	12/35 m	0.45 0.19–0.61	1.20 0.39–2.21	274 150–408	193 134–270	1.4
	OAE1c	17/70 m	0.65 0.15–1.40	2.31 0.11–4.91	365 55–820	138 39–327	2.6
	OAE1b	16/75 m	0.52 0.12–1.53	1.73 0.47–5.95	303 84–615	194 98–334	1.1
	OAE1a	7/7 m	1.24 0.40–3.31	2.75 0.11–8.28	205 25–323	88 21–170	2.3
OOJ	OAE1d	8/25 m	1.52 1.26–1.76	3.97 3.19–5.37	262 191–344	137 56–303	1.8
	OAE1c	11/16 m	0.48 0.32–0.79	1.41 1.19–1.67	350 171–516	89 29–220	3.9
	OAE1b	66/110 m	0.53 0–1.33	1.58 0–5.97	245 0–996	155 26–395	1.5

**Table 2** Dichloromethane extraction compounds of Bir M’Cherga Aptian–Albian source rocks

Section	Saturated HC (%)	Aromatic HC (%)	Resins (%)	Asphaltenes (%)	<i>n</i> -Alkanes ≤ C <sub>20</sub> %	C <sub>14</sub> ≤ <i>n</i> -alkanes ≤ C <sub>32</sub> %
ZAS	9	10	73	13	36	85
ZBB	14	6	56	1	50	98
AAS	13	5	56	9	–	–
OOB	32	4	60	7	64	98
OOJ	37	5	58	0	56	99

**Fig. 5** Chromatograms showing: **a** a non biodegraded hydrocarbons from dark shale; **b** biodegraded hydrocarbons of saturated dichloromethane extracted fraction showing a hump from organic poor light grey limestone of Bir M’Cherga source rocks (Corel Draw figure exported into jpeg format)

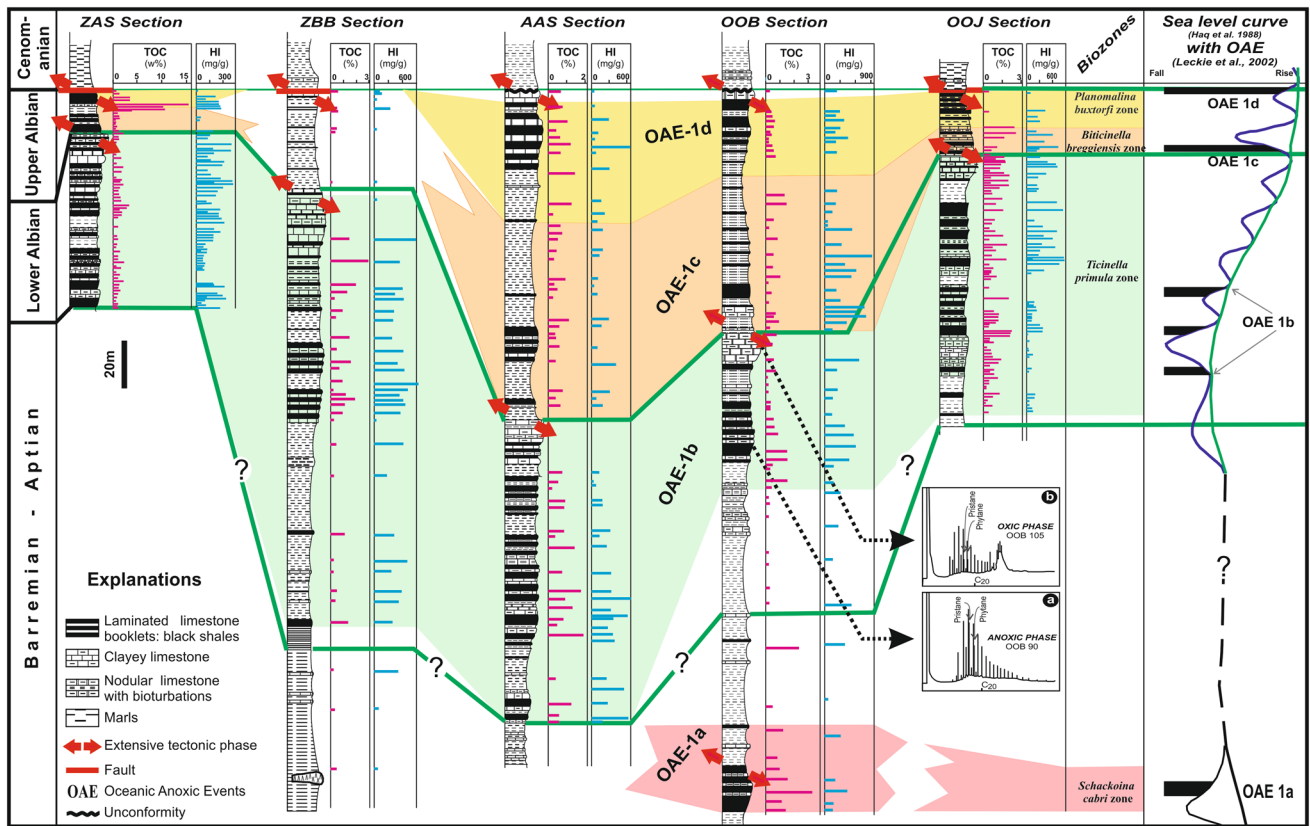


Fig. 6 Anoxic sub-events correlation with the organic geochemical parameters of Bir M'Cherga Aptian–Albian source rocks compared to their Western North Atlantic equivalents (Leckie et al. 2002) and the Vail sea level curve (Corel Draw figure exported into jpeg format)

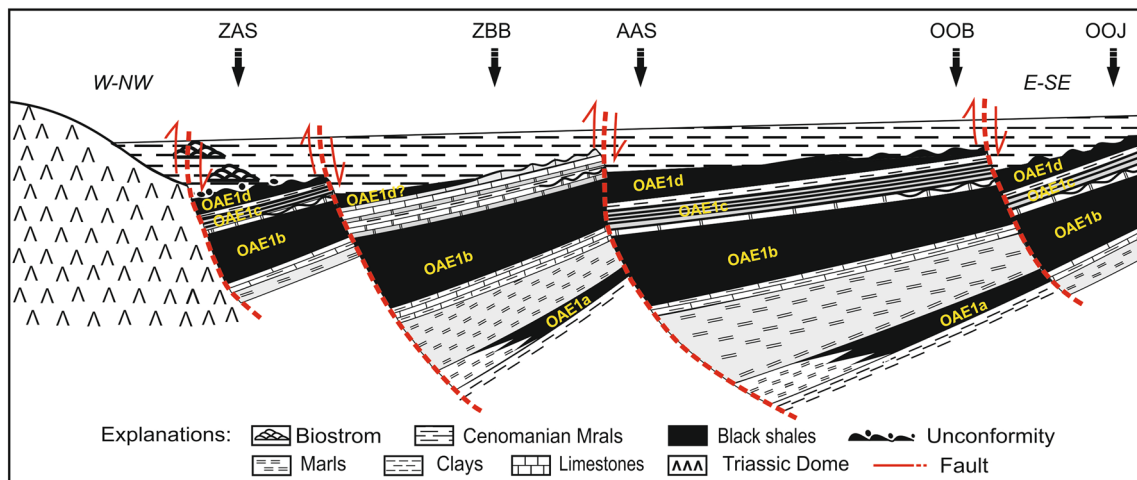
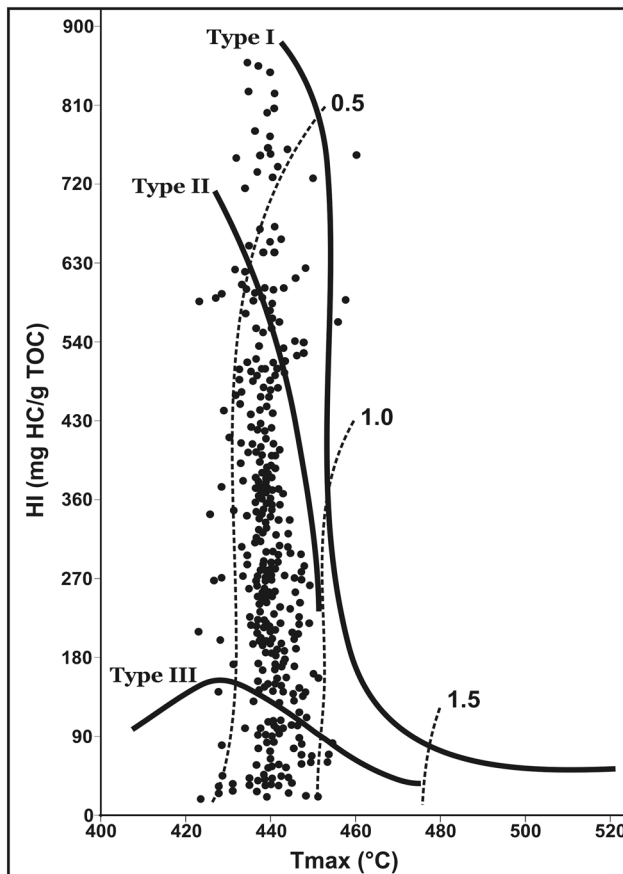


Fig. 7 Schematic NW-SE cross section showing black shales related to OAE1a, OAE1b, OAE1c, and OAE1d within tilted block guiding the Aptian–Albian sedimentation (Corel Draw figure exported into jpeg format)

western Tethyan (Arthur et al. 1985; Silvá et al. 1989; Bralower et al. 1994).

The third oceanic anoxic sub-event (OAE1c) appears at the lower Upper Albian and is identified by *Biticinella*

*breggiensis* biozone. It is represented by thin laminated black shales intercalated in a various thick marl series (15–72 m). A moderate organic content characterizes this sub-event with average contents of 0.55 wt% for TOC, 252 mg/g for HI and



**Fig. 8** HI/ $T_{max}$  diagram showing the representative points of Bir M'Cherga Aptian–Albian source rocks (Corel Draw figure exported into jpeg format)

1.81 kg HC/t for GHP. Their maximum values are recorded at ZAS section which are, respectively, 1.97, 608, and 7.37 (Table 1; Fig. 6). This sub-event was identified in central Italy (Silva et al. 1989), in Mexico (Bralower et al. 1994) in the western United States and in Australia (Bralower et al. 1994; Coccioni and Galeotti 1993; Haig and Lynch 1993; Erbacher et al. 1996).

The fourth oceanic anoxic sub-event (OAE1d) is located at the top of the Albian and was identified by *Planolites buxtoni* biozone and consists on black shales of about 12–50 m thick. A high organic matter content with an average of 2.02 wt% for TOC, 274 mg/g for HI and 8.34 kg HC/t for GHP, characterizes this oceanic sub-event. The exceptionally high values are recorded at (ZAS) section near the Jebel Zebbas Triassic outcrop. They measure 13.91 wt% for TOC, 436 for HI and 74.18 kg HC/t for GHP (Table 1; Fig. 6). In the rest of the basin, where more rich-marl facies dominated, the organic contents are moderate (about 1–2 wt% for TOC). This sub-event is well documented in Northern Thethys (Bornemann et al. 2017), Southern part of the Atlantic, Indian Ocean and in Eastern part of Pacific Ocean

(Br eh eret 1994; Erbacher et al. 1996; Wilson and Norris 2001).

## Unconventional petroleum system associated to Aptian–Albian anoxic sub-events

### Geodynamic factors controlling black shale deposition

In the Bir M'Cherga basin, the main three oceanic anoxic sub-events: OAE1a, OAE1b, and OAE1d are represented by black shales horizons. Only OAE1c is represented by thin beds of black shale within a thick marl sequence. Each black shale level is located within a filling second order fining and thickening upwards sequence and occurs with the highest transgressive sea level. A positive correlation between transgressive phase, illustrated by the Vail curve, the TOC and the HI peaks is shown by Fig. 6 where the anoxia is detected by the high contents of organic matter and the high sea level (Schlanger and Jenkyns 1976; Leckie et al. 2000). This positive correlation highlights the role of global factors in the oceanic anoxic sub-events determination. However, regional and local factors controlling the organic material preservation under anoxic conditions have certainly played an important role in the local expression of the oceanic anoxic sub-events. This is why the geodynamic context of the Bir M'Cherga black shales deposit was controlled by active distensive faults. Generated structures in horsts, grabens and tilted blocks (Fig. 7) induced by the Triassic halokinetic activity (Smati 1986; Perthuisot et al. 1988) had favor the deposition of black shales. Intermediate domain between subtidal (graben) and external platform (horst) constitutes the ideal environment of anoxia conditions to accumulate black shales. In this context, the Barremo–Aptian black shale levels of Oued Bou Hejba (OOB) are spotted on only near the resistant areas (Fig. 7).

At the Lower Albian, the anoxia spreads throughout the whole basin and characterizes a water depth higher than that of the Barremo–Aptian passage. The black shales are deposited on the entire basin with homogeneity of organic matter richness (maximum of 1–3 wt% TOC). During this period, the tectonic activity seems to affect neither the black shale distribution nor their organic richness. However, at the top of the sequence burrowed limestones, low organic matter content, express the transitional anoxic-to-oxic conditions before the advent of the terminal Lower Albian distensive tectonic phase. The latter phase reactivates old faults and creates relief inequalities (Fig. 7). The OAE1c occurred at the basal Upper Albian within the second sedimentary sequence is better expressed in the whole basin except in ZBB section. Finally, the OAE1d occurred at the terminal Upper Albian, records exceptionally organic-rich facies with about 14 wt% TOC at the resistant panels near the Triassic Jebel Zebbas area. Elsewhere, in the deepest areas of the



basin (Figs. 6, 7), this anoxic sub-event was expressed by moderate TOC contents with maximum 1–2 wt% TOC.

### Hydrocarbon potential productivities of black shale source rocks

The first point to consider in an area with exploitable oil potential production is the determination of the thermal maturity stage of the source rock. As it is shown in Figs. 8 and 9, the most  $T_{max}$  values range between 436 and 450 °C and the majority of representative points of samples are placed, between 0.5 and 1% vitrinite isoreflectance-bounding lines corresponding to the “oil window” as it is shown by HI/ $T_{max}$  diagram. This lead to consider Aptian–Albian source rocks as unconventional oil shale resources.

To characterize the hydrocarbon potential productivities of these unconventional oil shale resources, the variations of the following parameters are analyzed. Results are consigned in Tables 1 and 3. The hydrocarbon generation potential: HGP (S2+S1), the oil saturation index: OSI (S1 mg×100)/g TOC and the  $T_{max}$  values, are illustrated in parallel with TOC variations by Fig. 9. The average HGP ranges from 1.41 to 25.49 kg HC/t. The highest values are recorded in the sub-event OAE1d of the ZAS section (Table 1). Since the HGP represents the quantities of the free (S1) and potential (S2) hydrocarbons retained in source rocks, only S1 are able to flow once hydraulic fracturing has been implemented. OSI parameter ( $OSI = 100 \times S1/TOC$ ) can provide the existence of quantities of hydrocarbons likely to circulate. OSI exceeds 10% in mature source rock then it ranges between 50 and 70% for a saturated source rock as a result of cracking the majority or all its hydrocarbon generation potential. When reach by 100%, this creates target areas for shale oil exploitation. These areas are called “oil crossovers” (Jarvie 2012). The average OSI values of The Aptian–Albian Bir M’cherga basin range from 3 to 23% with a maximum exceeding 100% (Table 3; Fig. 9) that indicate oil saturation of the source rocks. The most dispersed values may be explained by secondary migration and existence of areas of oil accumulation. In fact Fig. 9 shows two “oil crossovers” areas in the two sections ZAS and OOB, where the series become condensate and affected by several faults (Fig. 9). Sections in the middle of the depression (AAS and OOB) do not show this oil crossover phenomenon, although the degree of thermal maturity is the highest in the basin. The average  $T_{max}$  values are, respectively, 442 °C and 440 °C, against 437 °C to 438 °C in ZAS, ZBB, and OOB sections (Table 3; Fig. 9). So the lack of oil crossover at AAS and OOB sections may be the result of a partial hydrocarbon expulsion.

The thermal transformation of organic matter that causes a source rock to generate petroleum is the transformation ratio (TR) which represents the percentage of organic matter that has been transformed into hydrocarbons between

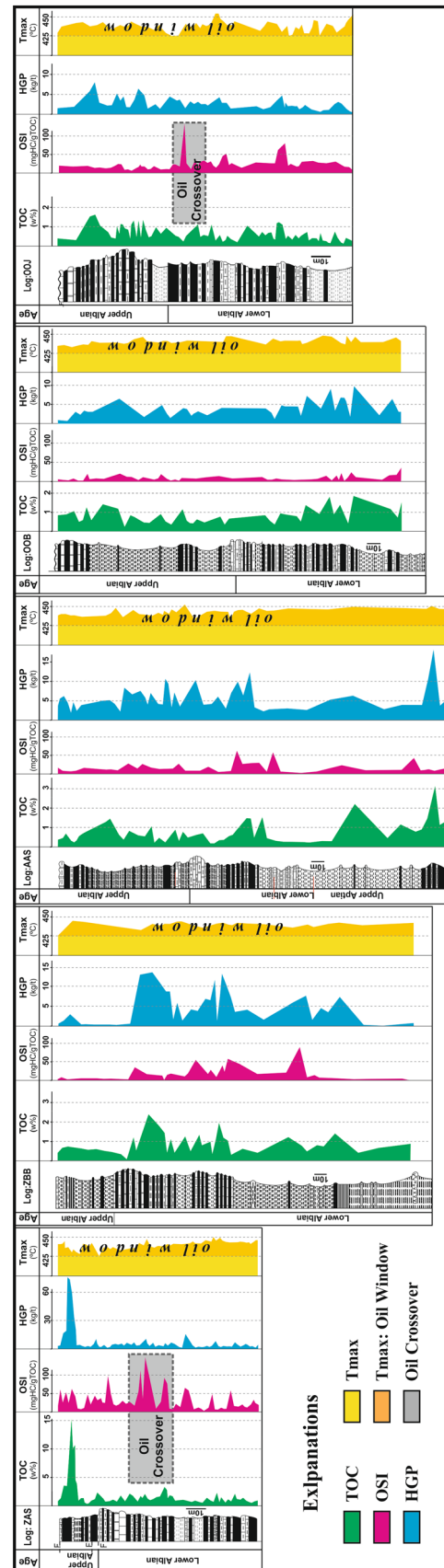


**Fig. 9** Variations of TOC, the hydrocarbon generation potential HGP (S2 + S1), the oil saturation index: OSI (S1 mg×100)/g TOC and  $T_{max}$  of Bir M’Cherga Aptian–Albian source rocks (Corel Draw figure exported into jpeg format)

**Table 3** Average oil saturation index: OSI ( $S1 \text{ mg} \times 100/\text{g}$  TOC), transformation ratio: TR (%) and  $T_{\text{max}}$  of Bir M'Cherga Aptian–Albian source rocks

Section	Sample Number	Sub-OAE	Average OSI %	Average TR %	Average $T_{\text{max}}$
ZAS	17	OAE1d	23 2–51	26	436
	14	OAE1c	19 0–42	62	438
	55	OAE1b	19 0–138	53	437
ZAS samples: 86		Average/section	20	47	437
ZBB	29	OAE1b	6 0–27	11	438
AAS	14	OAE1d	3 0–11	58	439
	11	OAE1c	3 0–13	49	442
	21	OAE1b	6 0–26	42	445
AAS samples: 46		Average/section	4	50	442
OOB	12	OAE1d	4 0–26	42	439
	17	OAE1c	4 0–11	23	441
	16	OAE1b	5 0–25	36	441
OOB samples: 53	8	OAE1a	5 1–10	57	443
		Average/section	4.5	40	441
	OOJ	8	OAE1d	5 1–11	30
OOJ	11	OAE1c	7 0–18	40	438
	66	OAE1b	11 0–133	48	437
	Total samples: 85		Average/section	8	40

the initial stage, where the organic matter was immature, and the final stage (present days), according to the following formula:  $TR = (HI_o - HI)/HI_o$  (Jarvie 2007). Knowing the type of organic matter,  $HI_o$  can be estimated to 475 °C for an organic material of a marine planktonic type II origin (Jarvie et al. 2007).

As it is shown in Table 3, the average value of TR/section ranges from 40 to 50%, then about 50–60% of the original hydrocarbons are still untransformed. The highest values of the TR are recorded in the center (50% in AAS section) and in NW ridge of the basin (47% in ZAS section) which show, respectively, the highest and the lowest maturity degree with, respectively, an average  $T_{\text{max}} = 442$  and 437 °C. This may be explained by the high maturity degree recorded in AAS section and the best quality of organic matter in ZAS section ( $HI/OI = 14$ ) as shown by Tables 1 and 3.

Those unconventional oil shale resources containing more than 50% of their initial hydrocarbon generation potential will be able to produce significant quantities of hydrocarbons

by hydraulic fracturing. As long as they are hosted in thick marl series preventing tertiary hydrocarbon migration to reservoir rocks, desorption of hydrocarbons may be achieved by the existence of natural fracturing and microfracturing as well as a juxtaposed rich organic bed alternated with the poor organic ones. In this context, dark shales may provide hydrocarbons by thermal cracking that would migrate into clear limestone facies constituting thin reservoirs into black shale source rocks. Taking account of all those characteristics, the Aptian–Albian petroleum source rock system can be qualified, according to the unconventional source rock classification established by Jarvie (2012), as an “unconventional oil shale hybrid systems with a combination of juxtaposed organic-rich and organic-lean intervals associated to open fractures”. It should be noted that the synsedimentary open fracture system which had been often reactivated during sedimentary filling cycles of the basin, may be considered as a weak path facilitating hydrocarbon secondary migration.

## Conclusions

During the Aptian–Albian period, the Bir M’Cherga basin had been the seat of important rich organic deposits consisting of black shales interbedded with marls and nodular limestones. The chronostratigraphy assigns these black shales to the four sub-events OAE1a, OAE1b, OAE1c, and OAE1d. The geological context in which these black shales are deposited, allowed understand the role played by local factors to boost the deposit of these organic-rich facies. This main role is attributed to synsedimentary tectonic phases that reactivated the old N–S and E–W basement faults, during three major tectonic phases occurring across: Aptian–Albian, Lower Albian–Upper Albian and Upper Albian–Cenomanian. The reactivation of these faults, combined with the Triassic halokinetic movements in Jebel Zebbas and Jebel Oust areas, marked the two extremities of this basin at this period, creating a particular architecture with horsts, grabens and tilted blocks. This resulted in a maximum collapse of the deep center of the basin with respect to the northwestern and southeastern wrinkles which were kept elevated during the entire Aptian–Albian interval. Sedimentation in this basin had oscillated between a subtidal deep sea in the grabens and an external platform on the top of horsts. In this context, black shales are formed in an intermediate zone connecting horsts and grabens. On the other hand, black shales formed near the paleo-high reliefs are more organic-rich facies than those deposited in the deep areas.

The geochemical and petrographic analysis of the organic matter show that the average TOC is 1.24, 0.7, 0.55, and 2.02 wt%, respectively, for OAE1a, OAE1b, OAE1c, and OAE1d with maximum values reaching, respectively, 3.13, 2.97, 1.97 and 13.91 wt%. The organic matter origin is overall homogeneous throughout the basin and is particularly an amorphous marine planktonic of type I and II origin with a small contribution of continental organic matter (about 5%). This organic matter quality produced significant hydrocarbon amounts with averages HGP/section ranging between 2 and 10 HC Kg/t rock. Considering the maturity stage that did not exceeded the “oil window”, these source rocks are defined as an unconventional shales oil resource system. The average transformation ratio TR of the organic matter is around 45%. Then more than a half of the initial HGP is still untransformed in the source rock. A good proportion of this HGP stored in the rock is in the form of free hydrocarbons. High proportions of the oil saturation index exceeding 100% create “oil crossover” areas in the two raised domains: ZAS and OOJ section.

The geological context combined to geochemical and petrological criteria lead to consider the Aptian–Albian source rocks in Bir M’Cherga basin as unconventional oil shale hybrid systems with a combination of juxtaposed organic-rich and organic-lean intervals associated with open fractures. Both, fracturing system and organic-rich interbedded

facies within black shales make possible hydrocarbon secondary migration and partial accumulations that have constituted the “oil crossover” areas. The thin poor-organic facies interbedded into black shales constitutes mini-reservoirs within the source rock, favoring a secondary migration through short distances by microfractures.

**Acknowledgements** This work was funded by the Ministry of Higher Education and Scientific Research of Tunisia. The authors thank the staff of the Research Center and Water Technologies in Borj Cedria (CERTe) for their technical support. Similarly, the authors are grateful to the staff of University of Orleans for their petrography analysis help. We are also grateful to Professor Chihi Lassad, Faculty of Sciences of Bizerte, for helping to improve the geodynamic part of this article.

**Open Access** This article is distributed under the terms of the Creative Commons Attribution 4.0 International License (<http://creativecommons.org/licenses/by/4.0/>), which permits unrestricted use, distribution, and reproduction in any medium, provided you give appropriate credit to the original author(s) and the source, provide a link to the Creative Commons license, and indicate if changes were made.

## References

- Arthur MA, Dean WE, Schlanger SO (1985) Variations in the global carbon cycle during the Cretaceous related to climate, volcanism, and changes in atmospheric CO<sub>2</sub>. *Carbon Cycle Atmos CO Natl Var Archean Present* 32:504–529. <https://doi.org/10.1029/GM032p0504>
- Ben Haj Ali N, Memmi L (2014) Northern Tunisian lower cretaceous stratigraphic approach using ammonites and microfaunas: a model for the tethys southern margin. In: STRATI 2013. Springer, Cham, pp 643–647. [https://doi.org/10.1007/978-3-319-04364-7\\_123](https://doi.org/10.1007/978-3-319-04364-7_123)
- Bertrand P, Pradier B (1993) “Optical methods applied to source rock study.” *Applied Petroleum Geochemistry*. Technip, Paris, pp 281–310
- Boltenhagen C (1981) Les séquences de sédimentation du Crétacé moyen en Tunisie centrale. *Actes du Premier Congrès National des Sciences de la Terre, Tunis*, pp 55–71
- Bolze J, Burolet F, Castany G (1952) Le Sillon tunisien. In: XIX<sup>e</sup> Congrès Géologique International, Monographies régionales, (2e Série: Tunisie), 5(2): 1–112
- Bornemann A, Erbacher J, Heldt M et al (2017) The Albian–Cenomanian transition and Oceanic Anoxic Event 1d—an example from the Boreal Realm. *Sedimentology* 64(1):44–65. <https://doi.org/10.1111/sed.12347>
- Bralower TJ, Arthur MA, Leckie RM et al (1994) Timing and paleoceanography of oceanic dysoxia/anoxia in the Late Barremian to Early Aptian (Early Cretaceous). *Palaios* 9(4):335–369. <https://doi.org/10.2307/3515055>
- Bréhéret JG (1994) The mid-Cretaceous organic-rich sediments from the Vocontian zone of the French Southeast Basin. In: *Hydrocarbon and petroleum geology of France*. Springer, Berlin, pp 295–320
- Burolet PF (1956) Contribution à l’étude stratigraphique de la Tunisie centrale. *Ann Mines Géol* 18:350
- Chihi L (1995) Les fossés néogènes à quaternaires de la Tunisie et de la mer pélagienne: leur étude structurale et leur signification dans le cadre géodynamique de la méditerranée centrale. *Dissertation, Université of Tunis II*
- Chikhaoui M, Turki MM (1995) Rôle et importance de la fracturation méridienne dans les déformations crétacées et alpines de



- la ‘zone des diapirs’ (Tunisie septentrionale). *J Afr Earth Sc* 21(2):271–280. [https://doi.org/10.1016/0899-5362\(95\)00066-3](https://doi.org/10.1016/0899-5362(95)00066-3)
- Coccioni R, Galeotti S (1993) Orbitally induced cycles in benthonic foraminiferal morphogroups and trophic structure distribution patterns from the Late Albian “Amadeus Segment” (Central Italy). *J Micropalaeontol* 12(2):227–239. <https://doi.org/10.1144/jm.12.2.227>
- Coccioni R, Galeotti S (1994) KT boundary extinction: Geologically instantaneous or gradual event? Evidence from deep-sea benthic foraminifera. *Geology* 22(9):779–782
- Dunham RJ (1962) Classification of carbonate rocks according to depositional texture. *American Association of Petroleum Geologists, Memoir 1*, pp 108–121
- Durand B (1993) Composition and structure of organic matter in immature sediments. In: *Applied petroleum geochemistry*: Paris, France. Editions Technip, pp 77–100
- Ellouz N (1984) Etude de la subsidence de la Tunisie atlasique orientale et de la mer pélagienne. Dissertation, Université Pierre et Marie Curie
- Erbacher J, Thurow J, Littke R (1996) Evolution patterns of radiolaria and organic matter variations: a new approach to identify sea level changes in mid-Cretaceous pelagic environments. *Geology* 24(6):499–502. [https://doi.org/10.1130/0091-7613\(1996\)024%3C0499:EPORAO%3E2.3.CO;2](https://doi.org/10.1130/0091-7613(1996)024%3C0499:EPORAO%3E2.3.CO;2)
- Espitalié J, Laporte JL, Madec M, Marquis F, Leplat P, Paulet J, Boutefeu A (1977) Méthode rapide de caractérisation des roches mères, de leur potentiel pétrolier et de leur degré d’évolution. *Revue de l’Institut français du Pétrole* 32(1):23–42. <https://doi.org/10.2516/ogst:1977002>
- Goy G (1979) Les “schistes cartons” (Toarcien Inferieur) du bassin de Paris. Dissertation, Université Pierre et Marie Curie, Paris
- Haig DW, Lynch DA (1993) A late early Albian marine transgressive pulse over northeastern Australia, precursor to epeiric basin anoxia: foraminiferal evidence. *Mar Micropaleontol* 22(4):311–362. [https://doi.org/10.1016/0377-8398\(93\)90020-X](https://doi.org/10.1016/0377-8398(93)90020-X)
- Illies JH (1981) Mechanism of Graben formation. *Tectonophysics* 73(1–3):249–266
- Jarvie DM (2012) Shale resource systems for oil and gas: part 2-Shale-oil resource systems. In Breyer JA (ed) *Shale reservoirs—giant resources for the 21st century: AAPG Memoir*, vol 97, pp 89–119
- Jarvie DM, Hill RJ, Ruble TE, Pollastro RM (2007) Unconventional shale-gas systems: the Mississippian Barnett Shale of north-central Texas as one model for thermogenic shale-gas assessment. *AAPG Bull* 91(4):475–499
- Jarvis I, Mabrouk A, Moody RTJ et al (2002) Late Cretaceous (Campanian) carbon isotope events, sea-level change and correlation of the Tethyan and Boreal realms. *Palaeogeogr Palaeoclimatol Palaeoecol* 188(3–4):215–248. [https://doi.org/10.1016/S0031-0182\(02\)00578-3](https://doi.org/10.1016/S0031-0182(02)00578-3)
- Jauzein A (1957) Carte géologique au 1/50 000 et notice explicative de Bir Mchergua, feuille n°28. Service Géologique de Tunisie, 40, Tunis
- Jenkyns HC, Brumsack HJ, Schlanger SO (1990) Stratigraphy, geochemistry and paleoceanography of organic carbon-rich Cretaceous sequences. *Cretaceous Resour Events Rhythms Backgr Plans Res* (304):1–75
- Laridhi-Ouazza N (1994) Etude minéralogique et géochimique des épisodes magmatiques mésozoïques et miocènes de la Tunisie. Dissertation, Université de Tunis
- Leckie DA, Schroder-Adams C, Rosenthal L, Wall JH (2000) An outcrop of the Albian Viking formation and a southerly extension of the Hulcorss/Harmon interval in west-central Alberta. *Bull Can Pet Geol* 48(1):30–42
- Leckie RM, Bralower TJ, Cashman R (2002) Oceanic anoxic events and plankton evolution: biotic response to tectonic forcing during the mid-cretaceous. *Paleoceanography* 17(3):1–13. <https://doi.org/10.1029/2001PA000623>
- Marie J, Trouve P, Desforges G, Dufaure P (1982) Nouveaux éléments de paléogéographie du Crétacé de Tunisie. *Cretac Res* 3(1–2):167–170. [https://doi.org/10.1016/0195-6671\(82\)90017-9](https://doi.org/10.1016/0195-6671(82)90017-9)
- Martinez C, Chikhaoui M, Truillet R et al (1991) Le contexte géodynamique de la distension albo-aptienne en Tunisie septentrionale et centrale: structuration éocrotacée de l’Atlas tunisien. *Ecolgae geologicae Helvetiae* 84: 61–82
- Memmi L (1989) Le Crétacé inférieur (Berriasien-Aptien) de Tunisie: biostratigraphie, paléogéographie et paléoenvironnements. Dissertation, Université Claude-Bernard
- Perthuisot V, Rouvier H, Smati A (1988) Style et importance des déformations antévaconiennes dans le Maghreb oriental; exemple du diapir du Jebel Sлата (Tunisie centrale). *Bulletin de la Société Géologique de France IV* 4(3): 391–398. <https://doi.org/10.2113/gssgfbull.IV.3.391>
- Raaf JFM, Althuis SP (1952) Présence d’ophites spilitiques dans le Crétacé des environs d’Enfidaville, XIXème Congr. Géol. Int. Alger, 2<sup>ème</sup> série, Tunisie
- Schieber J, Gordon B (2001) On the origin and significance of pyrite spheres in Devonian black shales of North America. *J Sediment Res* 71(1):155–166
- Schlanger SO, Jenkyns HC (1976) Cretaceous oceanic anoxic events: causes and consequences. *Geologie en mijnbouw* 55(3–4):179–184. <http://www.kngmg.nl/publicaties/njg.html>
- Silvá IP, Erba E, Tornaghi ME (1989) Paleoenvironmental signals and changes in surface fertility in Mid Cretaceous Corg-Rich pelagic facies of the Fucoid Marls (Central Italy). *Geobios* 22:225–236. [https://doi.org/10.1016/S0016-6995\(89\)80059-2](https://doi.org/10.1016/S0016-6995(89)80059-2)
- Sliter WV (1989) Aptian anoxia in the Pacific Basin. *Geology* 17(10): 909–912. [https://doi.org/10.1130/0091-7613\(1989\)017%3C0909:AAITPB%3E2.3.CO;2](https://doi.org/10.1130/0091-7613(1989)017%3C0909:AAITPB%3E2.3.CO;2)
- Smati A (1986) Les gisements de pb-ba et de fer du Djebel Sлата (Tunisie du centre-nord): minéralisations épigenétiques dans le Crétacé neritique de la bordure d’un diapir de Trias, gisements de Sidi Amor Ben Salem et de Sлата-fer. Dissertation, University of Paris 6
- Soua M (2016) Cretaceous oceanic anoxic events (OAEs) recorded in the northern margin of Africa as possible oil and gas shale potential in Tunisia: an overview. *Int Geol Rev* 58(3):277–320. <https://doi.org/10.1080/00206814.2015.1065516>
- Talbi R (1991) Etude géologique et géochimique des faciès riches en matière organique d’âge Albien du bassin de Bir M’Cherga (NE de Tunisie): déterminisme de leur genèse et intérêt pétrolier de la région. Dissertation, University of Tunis II
- Tissot BP, Welte DH (1984) “Kerogen: composition and classification.” *Petroleum Formation and Occurrence*. Springer, Berlin, pp 131–159
- Vail PR, Mitchum RM, Thompson S III (1977) Seismic stratigraphy and global changes of sea level, part 3: relative changes of sea level from coastal onlap. In: Payton CW (ed) *Seismic stratigraphy-applications to hydrocarbon exploration: american association of petroleum geologists memoir*, vol 26, pp 83–97
- Weissert H, Lini A, Föllmi KB, Kuhn O (1998) Correlation of Early Cretaceous carbon isotope stratigraphy and platform drowning events: a possible link? *Palaeogeogr Palaeoclimatol Palaeoecol* 137(3–4):189–203. [https://doi.org/10.1016/S0031-0182\(97\)00109-0](https://doi.org/10.1016/S0031-0182(97)00109-0)
- Wilson PA, Norris RD (2001) Warm tropical ocean surface and global anoxia during the mid-Cretaceous period. *Nature* 412(6845):425–429. <https://doi.org/10.1038/35086553>

## Affiliations

Rachida Talbi<sup>1</sup>  · Rached Lakhdar<sup>2</sup> · Amor Smati<sup>1</sup> · Reginal Spiller<sup>3</sup> · Raymond Levey<sup>4</sup>

<sup>1</sup> Georessources Laboratory, Research Center and Water Technologies (CERTÉ), Technopark of Borj-Cedria, BP 273, 8020 Soliman, Tunisia

<sup>2</sup> Sciences Faculty of Bizerte, Carthage University, Bassins Sédimentaires et Géologie du Pétrole (BSGP), 7000 Bizerte, Tunisia

<sup>3</sup> CEO Azimuth Energy, 1014, Bayou Island, Houston, TX 77063, USA

<sup>4</sup> Energy and Geoscience Institute, 423 Wakara Way, Suite 300, Salt Lake City, UT, USA